Journal of Hydroinformatics | 13.3 | 2011

Transient tests for locating and sizing illegal branches in pipe systems

S. Meniconi, B. Brunone, M. Ferrante and C. Massari

ABSTRACT

In pipe systems illegal branches can take away remarkable water resources with negative effects from both the economic and technical points of view. Difficulties in pointing out illegal branches by means of steady-state pressure and discharge measurements are mainly due to the fact that, of course, such systems are not active according to a regular time schedule. In this paper the possibility of using Transient Test-Based Techniques (TTBT) for the location and sizing of branches is shown. Specifically, tests carried out in different branched pipe systems at the Water Engineering Laboratory of the University of Perugia, Italy, show that TTBT allow us to detect branches irrespective of whether they are active or not. To improve the precision of the localization, arrival times of pressure waves are detected by means of wavelet analysis. Finally, a simple relation based on the water hammer theory is proposed to size the branch reliably.

Key words | apparent losses, illegal connections, pipe system, transient

S. Meniconi (corresponding author)
B. Brunone
M. Ferrante
C. Massari
Dipartimento di Ingegneria Civile ed Ambientale,
University of Perugia,
Via G. Duranti 93,
I-06125 Perugia,
Italy
E-mail: *silvia.meniconi@unipg.it*

NOMENCLATURE

The following symbols are used in this paper:

A	pipe area;
a	pressure wave speed;
C^-	negative characteristic line;
C^+	positive characteristic line;
D	pipe internal diameter;
DN	nominal diameter;
e	pipe thickness;
F	incident wave at the illegal branch;
f	wave reflected by the branch;
F_T	transmitted wave;
g	acceleration due to gravity;
k	damping factor;
j	wavelet scale;
h	pressure signal (piezometric head);
L	pipe length;
L'	distance between node V and the connection of the branch;
N	Reynolds number;
Nu	number of time increments in the wavelet transform;
Q	discharge;
RHDPEBV	Reservoir-High Density PolyEthylene Branch-Valve system;
RPLBV	Reservoir-PLastic Branch-Valve system;
t	time;
U	mean flow velocity;
W	wavelet transform;
α	generic pressure wave;
Δ	overpressure due to the maneuver;
δ	decrease of h due to the arrival of the pressure wave reflected by connection J at the measurement section;
χ	mother wavelet;
λ	Darcy–Weisbach friction factor;
ν	kinematic viscosity;

doi: 10.2166/hydro.2011.012

ψ	reflection coefficient;
ζ	generic signal.

Subscripts

b	branch;
E	node at the downstream end of the branch;
J	connection node between the main pipe and the branch;
J,b	initial node of the branch;
J,md	initial node of the main pipe immediately downstream J;
J,mu	end node of the main pipe immediately upstream J ;
k	experimental value corrected by considering the damping of pressure waves;
M	measurement section immediately upstream of the end valve;
m	main pipe;
R	reservoir;
V	maneuver valve.

Superscripts

t	time.

INTRODUCTION

"Out of sight, out of mind": this short sentence synthesizes properly the approach followed in the past by water utility managers who ignored leakage as well as viewed leakage control as a desperation measure. In the last 30 years, due to both the rarefaction of water resources and the greatly increased user demand, water utility managers realized that leakage detection is a "money-saving expense" and assigned a high priority to leak survey programs based on benefit–cost analysis (Journal of AWWA special issue 1979). Moreover, at present that leaks are costly also in terms of energy is a well-established idea (Colombo & Karney 2002). According to Lambert & Hirner (2000) and Lambert (2003), water losses can be divided into real and apparent or administrative losses. Real losses consist of water volumes that flow out of the system without reaching any user, whereas apparent or administrative losses concern water volumes reaching a user without being measured and/or paid for. Thus apparent losses may be due to illegal connections to the distribution network (water theft) or measurement errors. In many regions, not only in developing countries (Figure 1), but also in Europe – particularly in those regions in which the agricultural practices are greatly conditioned by water availability –unauthorized consumption is widely spread, drawing water from the supply pipe system.

Even if an exhaustive review of the available methods for leak and illegal consumption detection is beyond the scope of this paper, some basic concepts are reported in order to point out the interest in the proposed procedure. There are a number of criteria that a successful technique for leak and illegal consumption detection should address. Specifically, it should provide a rapid response and exhibit a significant degree of automation. Moreover, any reliable technique should require low skill and limited training to operate as well as exhibiting robustness in continual operation. In other

Figure 1 | (a) Illegal branch (Mfula 2007). (b) Draft inlet in Zambia (Chulu 2007).

words, the amount of and types of equipment employed, the time for setup and calibration, impact on operations, test procedure and duration and precision of results have to be considered (Flora *et al.* 1998) when a proper methodology has to be chosen. It is worth noting that the comparison between the water industry and the gas and oil industry is severe: well-instrumented pipelines and large investment in research as a routine make the difference (Misiunas *et al.* 2005).

In such a context, technologies based on the execution of transient tests (Transient Test-Based Techniques – TTBT) are very attractive. In fact, only pressure measurements are needed, very few tests allow us to locate both leaks and branches, and the duration of tests is of the order of a few minutes (Covas & Ramos 2010; Meniconi *et al.* 2010*b*). As a consequence, the survey costs and the interference with the functioning of the investigated system are negligible with respect to techniques based on steady-state measurements. With regard to the precision, the use of proper techniques to analyze the transient data allow us to localize leaks and branches with a precision less than few units per cent (Ferrante *et al.* 2007). These are the main reasons for the increasing success of TTBT, at least for supply pipe systems.

In the analysis of the time-history of the pressure measured during transient tests – hereafter referred to as the "pressure signal" – different approaches have been followed. Within the Inverse Transient Analysis (ITA) proposed by Liggett & Chen (1994), the pressure signal is simulated by means of unsteady flow differential equations and the location and size of leaks and branches are the unknowns of the problem. Alternatively, as will be shown below, the analysis can be focused on the discontinuities in the pressure signal due to the pressure waves reflected by leaks and branches. Such an analysis can be executed in the time domain (e.g. Jonsson & Larson 1992; Brunone & Ferrante 2001), in the frequency domain (e.g. Lee *et al.* 2005) or by means of wavelet functions (e.g. Stoianov *et al.* 2001; Al-Shidhani *et al.* 2003; Ferrante & Brunone 2003). Moreover, it can concern the first characteristic time of the pipe – the so-called short period analysis (e.g. Ferrante *et al.* 2009; Covas & Ramos 2010) – or it is extended to a longer period of time, the so-called long period analysis (e.g. Wang *et al.* 2002).

This paper is an extension of the one presented at the 10th International Conference on Computing and Control for the Water Industry – CCWI09 (Meniconi *et al.* 2009*b*), with further experimental tests carried out at the Water Engineering Laboratory (WEL) of the University of Perugia, Italy, as well as numerical simulations. Following this introduction, in the first part, the experimental setups at WEL are described. The second part deals with the short period analysis for the location of illegal branches by means of wavelet functions. In the third part, a methodology to evaluate the size of the branches is proposed. Finally, the main results are synthesized in the conclusions.

EXPERIMENTAL SETUPS

Experimental tests were executed in two different pipe systems at WEL (Table 1): the Reservoir-PLastic-Branch-Valve system (RPLBV system, Figure 2(a)) and the Reservoir-High Density PolyEthylene Branch-Valve system (RHDPEBV system, Figure 2(b)). In both systems, the main pipe is a High Density PolyEthylene (HDPE) pipe (internal diameter $D_m = 93.3$ mm, nominal diameter DN110, thickness $e_m = 8.1$ mm, with the subscript m referring the quantities to the main pipe). It is supplied by an upstream constant head reservoir (hereafter denoted "node R") and a maneuver valve – a DN50 ball valve (hereafter denoted "node V") – is placed at the downstream end section. Differences between the two pipe systems concern the length of the main pipe, L_m, and the characteristics of the branch (material, diameter, thickness, length and external constraints) as well as the distance,

Table 1 | Pipe system characteristics

		Characteristics of the branch			
System	Length of the main pipe L_m (m)	Material	D_b (mm)	L_b (m)	L' (m)
RPLBV	164.93	Plastic	22.3	36.30	102.70
RHDPEBV	259.60	High density polyethylene	93.3	116.78	61.78

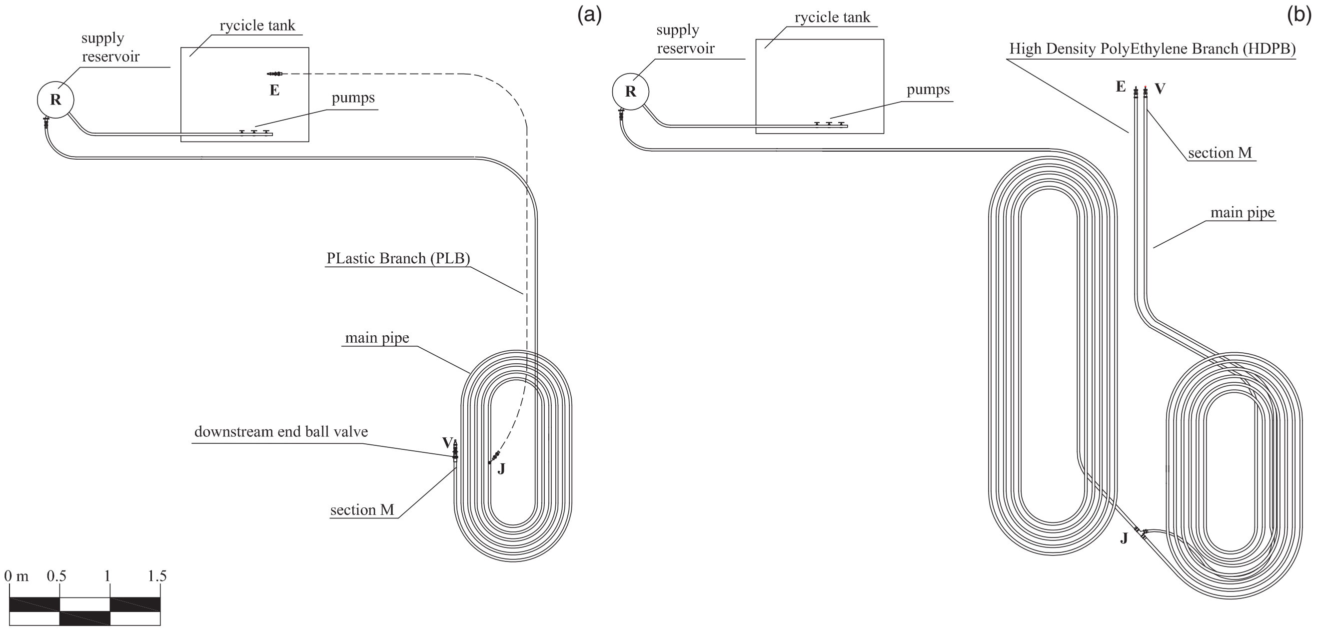

Figure 2 | Experimental setups: (a) RPLBV system and (b) RHDPEBV system.

L', from the connection between the main pipe and the branch – hereafter denoted "node J" – to node V (Table 1 and Figure 3). Precisely, for the RPLBV system (Figure 2(a)), $L_m = 164.93$ m and a PLastic Branch (PLB – $L_b = 36.30$ m, $D_b = 22.3$ mm and $e_b = 4$ mm, with the subscript b referring the quantities to the branch) is connected to the main pipe at a distance $L' = 102.70$ m. To simulate real pipe systems, such a branch is installed precariously (Figure 4(a)).

In order to simulate both active and inactive branches, a DN20 ball valve is installed at the downstream end of the branch (node E in Figure 2(a)).

In the RHDPEBV system (Figure 2(b)), $L_m = 259.60$ m and the branch is an HDPE pipe ($L_b = 116.78$ m, $D_b = D_m$ and $e_b = e_m$) that is connected to the main pipe at $L' = 61.78$ m (Figure 4(b)). In such a system, node E is a dead end.

The characteristics of the laboratory setups have been chosen in order to simulate real systems in term of length, diameter and flow conditions (i.e. turbulent regime). With respect to the short metallic small diameter pipes used in other laboratories, the small values of the pressure wave speed as well as the length of the installed pipes allow us to analyze in detail the interaction between a pressure wave and the system anomalies, such as illegal branches.

For both systems, pressure signals are acquired by piezo-resistive transducers, with a frequency acquisition of 1024 Hz, at sections M – placed immediately upstream of the maneuver valve V – E and J (Figure 3). The steady-state discharge is measured by means of a magnetic flowmeter.

LOCALIZATION OF ILLEGAL BRANCHES AND EVALUATION OF THEIR FUNCTIONING CONDITIONS

RPLBV system

Figure 5 compares the pressure signal, h_M^t – with the superscript t indicating the time and the subscript M referring the quantities to section M – during two transient tests generated by the fast and complete closure of valve V. Such tests are executed with the same steady-state discharge, $Q^0_{j,\mathrm{md}}$ ($= 3.429$ l/s), with the superscript 0 indicating the initial conditions and the subscript md referring the quantities to the segment of the main pipe downstream of node J. In the first test (continuous line in Figure 5) the branch is active, whereas in the second test (dashed line) it is inactive. In both

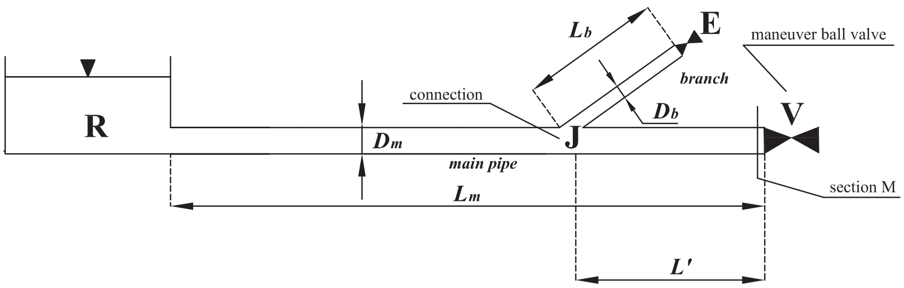

Figure 3 | Experimental setup definition sketch.

tests, the branch gives rise to reflected waves whose arrival times at section M allow its detection.

Revealing these times can be properly and precisely done by means of the wavelet transform that improves the precision of the localization, with respect to the time domain analysis (Stoianov *et al.* 2001; Al-Shidhani *et al.* 2003; Ferrante & Brunone 2003). The wavelet transform, W, of a discontinuous generic signal, ζ, sampled at a constant frequency for a limited number of time increments Nu ($\zeta(i\Delta t)$, $i=0, \ldots, Nu$-1, with $\Delta t=$ sampling period) can be defined as

$$W\zeta(i\Delta t) = \frac{1}{2^j}\sum_{m=0}^{Nu-1}\zeta(m\Delta t)\chi\frac{(m-i)\Delta t}{2^j} \tag{1}$$

where 2^j is the scale parameter, with the wavelet scale $j=1, 2, \ldots, I$, $I<\log_2 Nu$ and the mother wavelet, $\chi(t)$, is defined by the following expression:

$$\chi(t) = \begin{cases} 0 & |t|\geq 1 \\ \chi(-t) & 0\leq t<1 \\ -24t^2-16t & -0.5\leq t<0 \\ 8(t+1)^2 & -1<t<-0.5 \end{cases} \tag{2}$$

which is an approximation of the first derivative of the Gaussian function (Mallat & Zhong 1992). Precisely, in correspondence to singularities in the pressure signal, i.e. to the passage of waves through section M, the wavelet transform, W, is marked by maximum local moduli that organize themselves into chains (Ferrante *et al.* 2007). Such chains are indicated by dashed–dotted lines in Figures 6(b) and 7(b) that show the W of the pressure signal in the case of active (Figure 6(a)) and inactive branches (Figure 7(a)), respectively. In particular, scrutiny of Figures 6(b) and 7(b) reveals three singularities during the first characteristic time. The first singularity, i.e. the pressure rise, Δ_M, occurring at $t_V=0.200$ s (indicated by capital V in Figures 6(b) and 7(b)), is due to the arrival at section M of the wave generated by the maneuver. The second discontinuity, i.e. the pressure decrease, δ_M, at $t_J=0.781$ s, and the third one, at $t_R=1.117$ s, are caused by the waves reflected by the junction J and the reservoir R, respectively. It is worth noting that δ_M is approximately double the wave reflected by the connection J because at t_J the maneuver valve is completely closed. On the basis of such times, both the location of the illegal branch and the pressure wave speed, a_m, of the main pipe can be evaluated by the following relationships:

$$L' = \frac{t_J - t_V}{t_R - t_V}L_m \tag{3}$$

$$a_m = \frac{2L_m}{t_R - t_V}. \tag{4}$$

The relative error in evaluating L' is equal to 1.8%, in the case of both active and inactive branches, and the resulting value of a_m is 359.72 m/s. It is worth noting that, according to Equations (3) and (4), the localization of singularities and the evaluation of the pressure wave speed coincide with the evaluation of times at which pressure waves pass through the measurement section.

In order to determine the functioning conditions of the branch, the second characteristic time has to be analyzed. To evaluate the causes of the discontinuities in such a period of time, the numerical simulation of h_M^t by the Method Of Characteristics (MOC, see the Appendix) could be advantageous. To calculate a_b, an essential parameter in MOC, a transient test is generated by the total and complete closure of the valve at node E and pressure signals are acquired at sections E, J and M (Figure 8). In this figure, some disturbances in h_E^t can be noted, immediately after the end of the maneuver, due to the mentioned precarious installation of the

Figure 4 | Connection between the main pipe and the branch: (a) RPLBV system and (b) RHDPEBV system. In the square the connection node is highlighted.

branch. These evident disturbances have been reflected in the wavelet analysis of h_E^t (Figure 9(b)) and h_J^t (Figure 9(d)). However, some chains are clearly pointed out by such an analysis: in particular, the first chains of Figure 9(b) and (d) that are due to the arrival of the wave generated by the maneuver at sections E and J, respectively. Consequently,

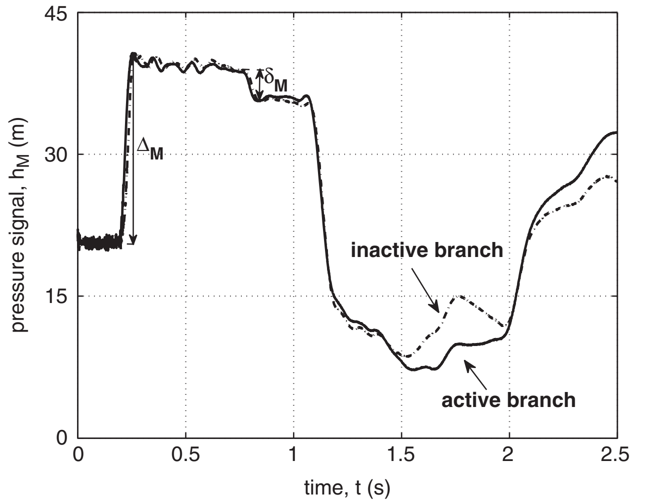

Figure 5 | RPLBV system: pressure signal at section M in the case of active (continuous line) and inactive (dashed line) illegal branch.

the value of a_b ($=79.89$ m/s) is determined by means of the following equation:

$$a_b = \frac{2L_b}{t_J - t_E}. \tag{5}$$

The numerical simulation by MOC is reported in Figure 10. Such a figure shows that the wave reflected at section E causes a different singularity at $t_E = 1.690$ s dependent on the functioning conditions in the branch. Precisely, in the case of an active branch such a singularity is a reduction

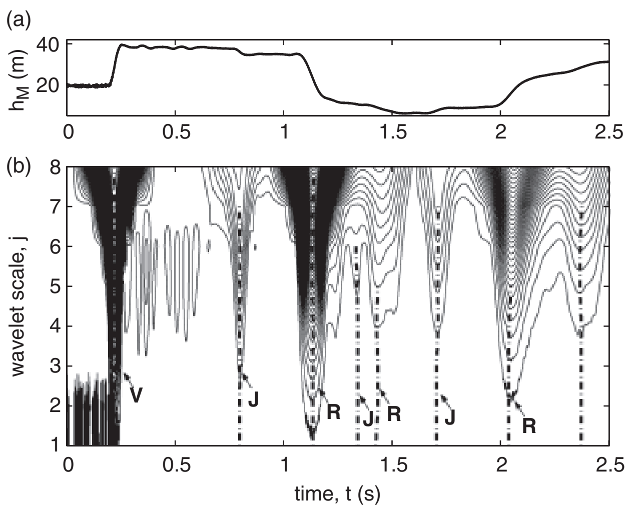

Figure 6 | RPLBV system: (a) pressure signal at section M in the case of active illegal branch (Figure 5) and (b) relative wavelet transform.

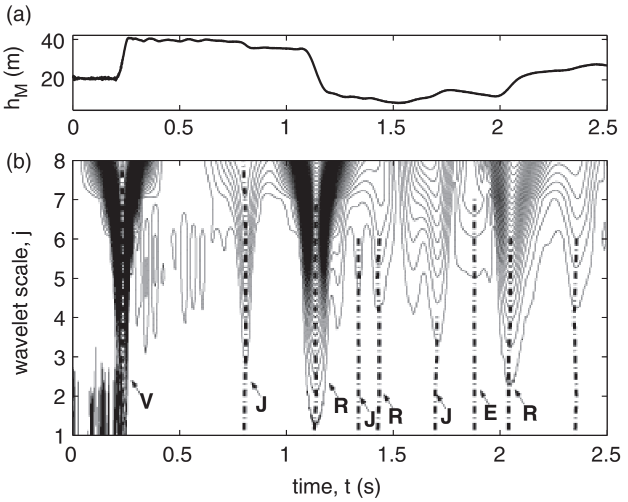

Figure 7 | RPLBV system: (a) pressure signal at section M in the case of inactive illegal branch (Figure 5) and (b) relative wavelet transform.

of 2.56 m, whereas in the case of an inactive branch it is an increase of 5.21 m.

In Figure 11 the pressure signals acquired at section E during the same transient test of Figure 5 are shown. Even if such data are not available in field tests, they allow us to better understand the investigated phenomenon. In fact, pressure signals acquired at node E are significantly different according to the boundary condition at section E. Precisely, when the branch is active and then the valve at node E is open, the pressure signal is almost constant. In contrast, in the case of an inactive branch, since the valve is closed, significant reflection phenomena occur.

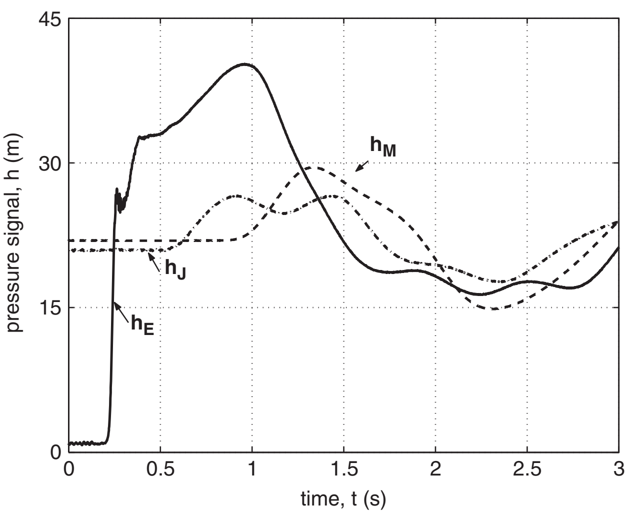

Figure 8 | RPLBV system: pressure signal at sections E, J and M acquired during a transient test generated by the maneuver of the valve installed at node E.

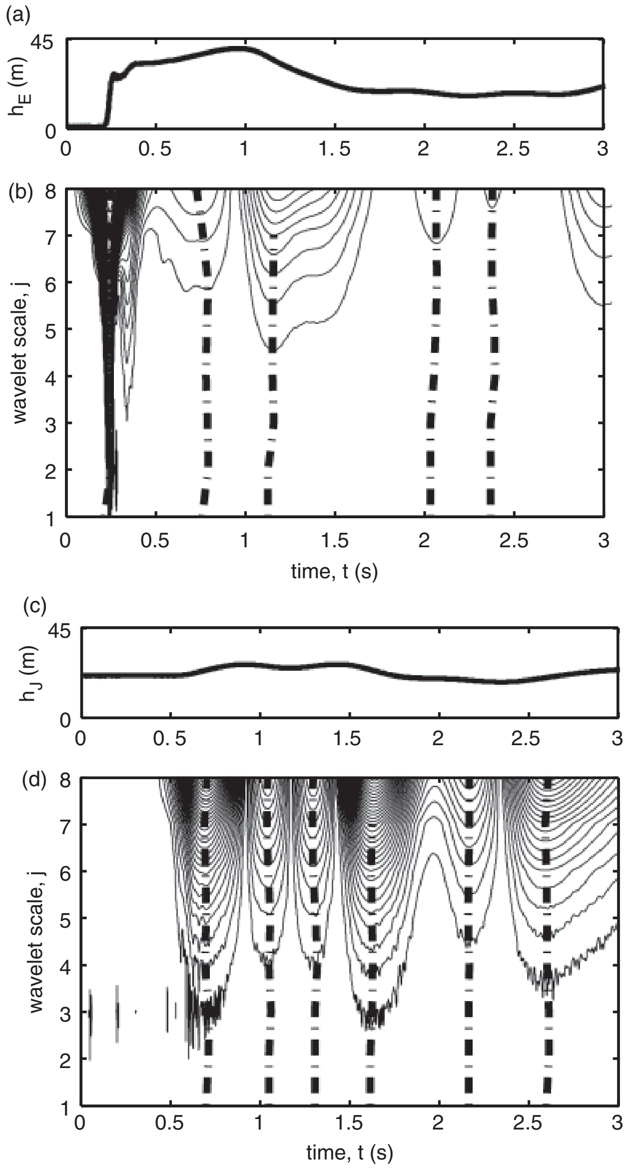

Figure 9 | RPLBV system: (a) pressure signal at section E, h_E, of Figure 8, (b) relative wavelet transform, (c) pressure signal at section J, h_J, of Figure 8 and (d) relative wavelet transform.

RHDPEBV system

An example of h_M^t during a transient test generated by the total and fast closure of valve V, with $Q_{J,md}^0 = 2.927$ l/s, is shown in Figure 12(a); in Figures 12(b) and 13(b) the relative numerical simulation and the wavelet analysis are reported, respectively. Since in the RHDPEBV system the value of the pressure wave speed is much larger than the one of the RPLBV system, the pressure wave travel time is smaller. As

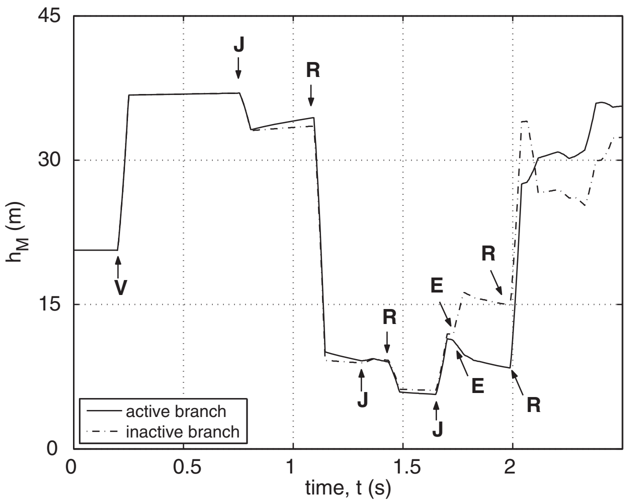

Figure 10 | RPLBV system: numerical simulation of pressure signal at section M in the case of active (continuous line) and inactive (dashed line) branch.

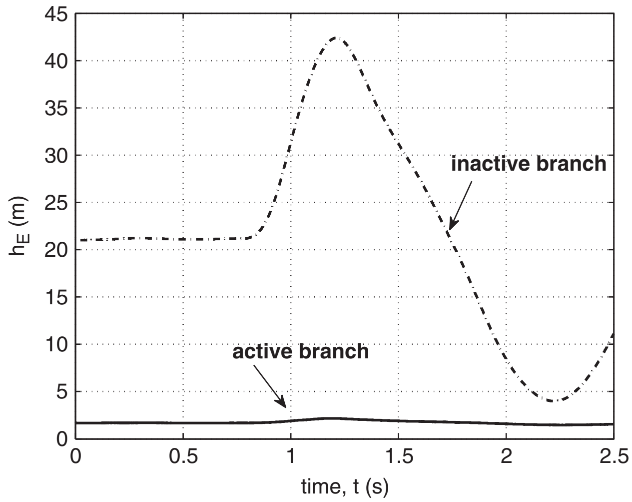

Figure 11 | RPLBV system: pressure signals at section E during the transient test of Figure 5.

a consequence, after the arrival of the pressure wave generated by the maneuver at $t_V = 0.237$ s, two waves reflected at node J arrive at section M one after the other. Such singularities are detected by the W at $t_{J'} = 0.582$ s and $t_{J''} = 0.912$ s, respectively. Moreover, the chain in the W at $t_E = 1.228$ s is due to the sudden and sharp increase caused by the reflection of the pressure wave at the dead end at section E. Finally, the singularity at $t_R = 1.695$ s corresponds to the arrival of the pressure wave reflected by the reservoir. By means of Equation (3), it is possible to evaluate L' with a relative error equal to 0.57%.

SIZING OF ILLEGAL BRANCHES BY SIMPLE MODELS

Within TTBT, simple numerical models, simulating the interaction between an illegal branch and a pressure wave, are advantageous in practical applications because they allow

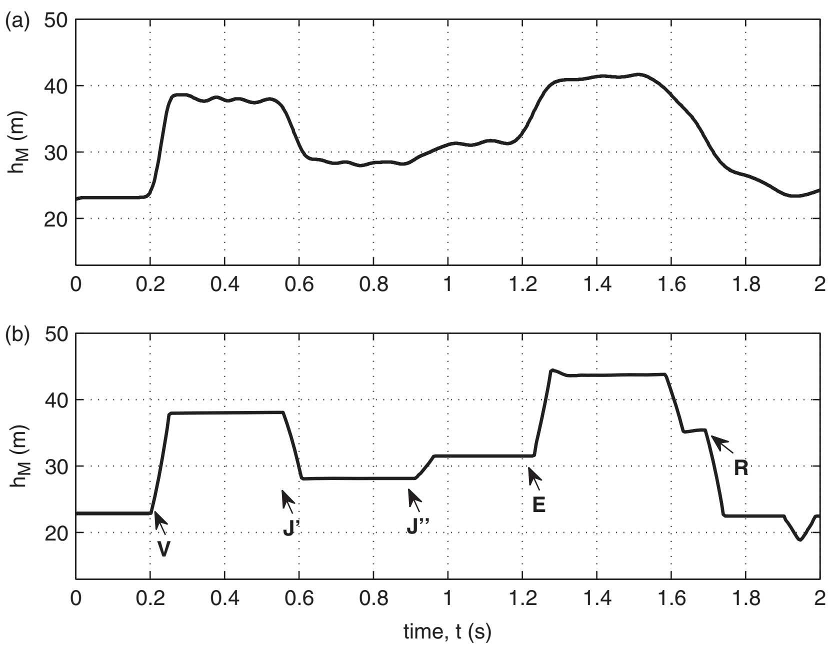

Figure 12 | RHDPEBV system: (a) pressure signal at section M and (b) relative numerical simulation.

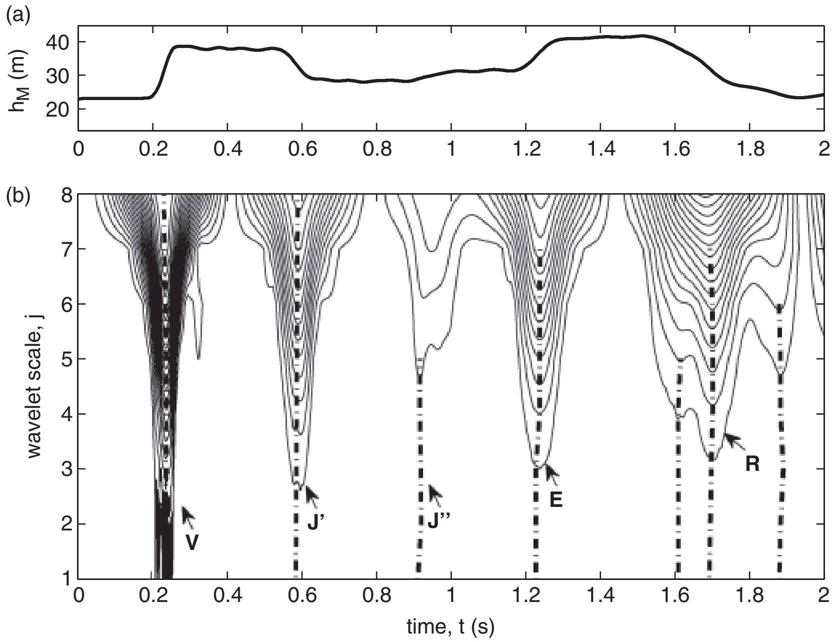

Figure 13 | RHDPEBV system: (a) pressure signal at section M and (b) relative wavelet transform.

sizing the branch straightforwardly. Such models are based on the assumptions of instantaneous closure and negligible friction losses. A prompt and useful tool to size branches is based on the evaluation of the reflection coefficient, ψ, defined as

$$\psi = \frac{f_J}{F_J} \tag{6}$$

with f = reflected wave and F = incident wave at node J. Under the above-mentioned hypotheses, the value of the ratio A_b/a_b is given by the following expression (Swaffield & Boldy 1993):

$$\frac{A_b}{a_b} = -\frac{\psi \cdot \frac{2A_m}{a_m}}{1+\psi}. \tag{7}$$

Since the characteristics of the main pipe are known and then the ratio A_m/a_m, in Figure 14 the behavior of A_b/a_b vs. ψ is reported according to Equation (7), in the range $0 < A_b/a_b < 2 \times 10^{-5}$. The resulting curve can be used for estimating the ratio A_b/a_b on the basis of the experimental value of the reflection coefficient that can be extracted from the pressure signal, h_M^t:

$$\psi_M = \frac{0.5\delta_M}{\Delta_M}. \tag{8}$$

The resulting values of ψ_M are -0.095 for the RPLBV system and -0.295 for the RHDPEBV system (Figure 14). Assuming in Equation (7)), $\psi = \psi_M$, for the RPLBV system $A_b/a_b = 3.97 \times 10^{-6}$ ms and for the RHDPEBV system $A_b/a_b = 1.59 \times 10^{-5}$ ms. The high relative errors in the evaluation of A_b/a_b (18.71% and 16.26%, respectively) are due to the differences between the incident pressure wave to junction J, F_J, and Δ_M and between the reflected pressure wave, f_J, and $0.5\delta_M$. Such differences can be ascribed to the damping of pressure waves, traveling from node V to node J and vice versa, mainly due to pipe viscoelasticity and unsteady friction (Meniconi *et al.* 2009*a*). According to Ramos *et al.* (2004) and Soares *et al.* (2008), such a damping has been estimated experimentally in a straight pipe. In particular, as described in Meniconi *et al.* (2010*a*), the damping of pressure waves traveling between two generic sections in the main pipe at a distance L^* can be measured by considering the damping factor k^t defined as

$$k^t = \frac{\alpha(t - L^*/a_m) - \alpha(t)}{L^*} \tag{9}$$

where α = generic pressure wave. The tests carried out show that, for given pipe material and characteristics, the damping factor k^t depends mainly on the inertial forces, i.e. on the Reynolds number, $N_m^t = \Delta U_m^t D_m/\nu$, where ΔU_m^t is the velocity

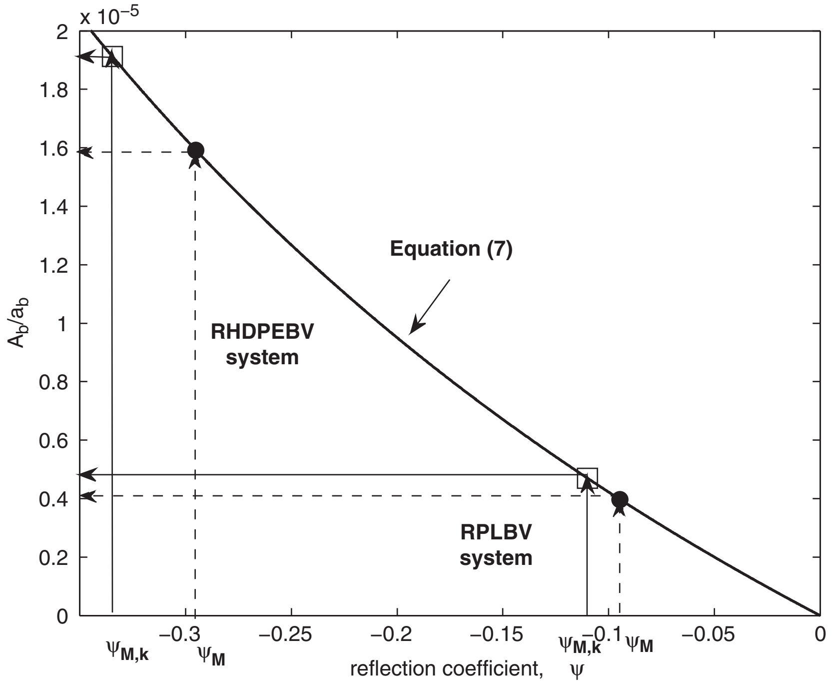

Figure 14 | The reflection coefficient of the illegal connection vs. A_b/a_b.

change associated to the pressure wave and ν is the kinematic viscosity of the fluid. The best fitting curve of k^t is given by the following relationship:

$$k^t = 4{\cdot}10^{-7} N_m^t. \tag{10}$$

If the experimental reflection coefficient, ψ_{M}, is corrected by considering k^t, the modified reflection coefficient is

$$\psi_{M,k} = \frac{0.5\delta_M + k^{t_f} L'}{\Delta_M - k^0 L'}. \tag{11}$$

The estimated values of $\psi_{\mathrm{M},k}$ ($=-0.110$ for the RPLBV system and $=-0.335$ for the RHDPEBV system) provide values of $A_{\mathrm{b}}/a_{\mathrm{b}}$ very close to the actual ones, with relative errors equal to 3.92% for the RPLBV system and 0.62% for the RHDPEBV system.

About the extension of the obtained results to pipe systems of different characteristics, a distinction has to be made between elastic and viscoelastic pipes. Precisely, for elastic pipes – where the damping is mainly due to unsteady friction and its effects are negligible in the first characteristic time – Equation (7) can be used reliably. In contrast, for viscoelastic pipes – where the damping strongly depends on the mechanical properties – there are three practical solutions: (i) to carry out tests to evaluate k^t, (ii) to execute tests at low values of the Reynolds number, where the damping is less important (Meniconi et al. 2010a) and (iii) to generate pressure waves by means of the Portable Pressure Wave Maker device (Brunone et al. 2008; Meniconi et al. 2011) that allows us to carry out tests starting from hydrostatic conditions.

CONCLUSIONS

The experimental results obtained at the Water Engineering Laboratory for two different branched pipe systems confirm the possibility of using transient tests as a powerful tool for the diagnosis and survey of pipe systems. Specifically, the location and sizing of illegal branches can be performed irrespective of whether they are active or not.

A precise location of illegal branches can be obtained by analyzing the pressure signals by means of the wavelet transform. The size of the branch is strongly related to the reflection coefficient of the connection of the illegal branch. Analytical values of the reflection coefficient are compared with the experimental ones and a good agreement is obtained when the damping of pressure waves in the main pipe is taken into account.

ACKNOWLEDGEMENTS

This research has been supported by the Italian Ministry of Education, University and Research (MIUR) under the Project of Relevant National Interest "Innovative criteria for the sustainable management of water resources in the water distribution systems". The support of A. Cirimbilli in the laboratory activity is highly appreciated.

REFERENCES

Al-Shidhani, I., Beck, S. B. M. & Staszewsky, W. J. 2003 Leak monitoring in pipeline networks using wavelet analysis. *Key Engng. Mater.* **245–246**, 51–58.

Brunone, B. & Ferrante, M. 2001 Detecting leaks in pressurised pipes by means of transients. *J. Hydraul. Res.* **39**(5), 539–547.

Brunone, B., Ferrante, M. & Meniconi, S. 2008 Portable pressure wave-maker for leak detection and pipe system characterization. *J. AWWA* **100**(4), 108–116.

Chulu, E. 2007 *Water Loss Management Problem at Kafubu Water and Sewerage Company in Ndola, Zambia*. Masters thesis, Urban Water Engineering, University of Perugia, Perugia.

Colombo, A. & Karney, B. W. 2002 Energy and costs of leaky pipes: towards comprehensive picture. *J. Wat. Res. Plan. Mngmnt.* **128**(6), 441–450.

Covas, D. & Ramos, H. 2010 Case studies of leak detection and location in water pipe systems by inverse transient analysis. *J. Wat. Res. Plan. Mngmnt.* **136**(2), 248–257.

Ferrante, M. & Brunone, B. 2003 Pipe system diagnosis and leak detection by unsteady-state tests. 2. Wavelet analysis. *Adv. Wat. Res.* **26**, 107–116.

Ferrante, M., Brunone, B. & Meniconi, S. 2007 Wavelets for the analysis of transient pressure signals for leak detection. *J. Hydraul. Engng.* **133**(11), 1274–1282.

Ferrante, M., Brunone, B. & Meniconi, S. 2009 Leak detection in branched pipe systems coupling wavelet analysis and a Lagrangian model. *J. Wat. Supply Res. Tech. – AQUA* **58**(2), 95–106.

Flora, J. D., Glauz, W. D., & Hennon, J. 1998 *Results of Range-finding Testing of Leak Detection and Leak Location Technologies for Underground Pipelines*. API Publication no. 346. API, Washington, DC.

Jonsson, L. & Larson, M. 1992 Leak detection through hydraulic transient analysis. In: *Proc. Int. Conf. on Pipeline Systems, Manchester, UK* (Coulbeck, B. & Evans, E. (Eds.)). pp 273–286. BHR Group, Manchester.

Journal of AWWA 1979 Special issue "Leak detection: a money-saving expense" (Theme introduction). *J. AWWA* **71**(2), 51.

Lambert, A. 2003 Assessing non revenue water and its components: a practical approach. *Water 21*, (August) pp 50–51.

Lambert, A. & Hirner, W. 2000 Losses from water supply systems: standard terminology and recommended performance measures. *IWA The Blue Pages*, pp 1–13. IWA, London.

Lee, P. J., Vitkovsky, J. P., Lambert, M. F., Simpson, A. R. & Liggett, J. A. 2005 Frequency domain analysis for detecting pipelines leaks. *J. Hydraul. Engng.* **131**(7), 596–604.

Liggett, J. A. & Chen, L. C. 1994 Inverse transient analysis in pipe networks. *J. Hydraul. Engng.* **120**(8), 934–955.

Mallat, S. G. & Zhong, S. 1992 Characterization of signals from multiscale edges. *IEEE Trans. on Pattern Analysis and Machine Intelligence.* **14**, 710–732.

Meniconi, S., Brunone, B. & Ferrante, M. 2009*a* In-line partially closed valves: how to detect by transient tests. In: *Proc. World Environmental & Water Resources Congress (EWRI09) , 17–21 May, Kansas City, MO* (Starrett, S. (Ed.)). pp 135–144. ASCE, Reston, VA. Doi: 10.1061/41036(342)14.

Meniconi, S., Brunone, B. & Ferrante, M. 2010*a* In-line pipe device checking by short period analysis of transient tests. *J. Hydraul. Engng.* DOI: 10.1061/(ASCE)HY.1942-7900.0000309.

Meniconi, S., Brunone, B., Ferrante, M. & Massari, C. 2009*b* Detection of illegal branches in pipe systems: a fast and reliable method. In: *Proc. 10th Int. Conf. on Computing and Control for the Water Industry (CCWI09), 1–3 September, Sheffield, UK* (Boxall, J. & Maksimovic, C. (Eds.)). pp 72–89. CRC Press, Boca Raton, FL.

Meniconi, S., Brunone, B., Ferrante, M. & Massari, C. 2010*b* Potential of transient tests to diagnose real supply pipe systems: What can be done with a single extemporary test. *J. Wat. Res. Plan. Mngmnt.* **137**, DOI: 10.1061/(ASCE)WR.1943-5452.0000098

Meniconi, S., Brunone, B., Ferrante, M. & Massari, C. 2011 Small amplitude sharp pressure waves to diagnose pipe systems. *Wat. Res. Mngmnt.* **25**(1), 79–96.

Mfula, B. 2007 *The Impact of Leakage and Leak Management in Water Supply Systems. The Case of Chingola, Zambia*. Masters thesis, Urban Water Engineering, University of Perugia, Perugia.

Misiunas, D., Vitkovsky, J. P., Olsson, G., Simpson, A. R. & Lambert, M. F. 2005 Pipeline break detection using pressure transient monitoring. *J. Wat. Res. Plan. Mngmnt.* **131**(4), 316–325.

Ramos, H., Covas, D. & Borga, A. 2004 Surge damping analysis in pipe systems: modelling and experiments. *J. Hydraul. Res.* **42**, 413–425.

Soares, A., Covas, D. & Reis, L. 2008 Analysis of PVC pipe-wall viscoelasticity during water hammer. *J. Hydraul. Engng.* **134**(9), 1389–1394.

Stoianov, I., Karney, B. W., Covas, D., Maksimovic, C. & Graham, N. 2001 Wavelet processing of transient signals for pipeline leak location and quantification. In: *Proc. Int. Conf. on Computing and Control for the Water Industry, 3–5 September, Leicester, UK* (Coulbeck, B. & Rance, J. (Eds.)). pp 65–76.

Swaffield, J. A. & Boldy, A. 1993 *Pressure Surge in Pipe and Duct Systems*. Gower Press, Ashgate, Farnham.

Wang, X. J., Lambert, M. F., Simpson, A. R., Liggett, J. & Vitkovsky, J. P. 2002 Leak detection in pipelines using the damping of fluid transients. *J. Hydraul. Engng.* **128**(7), 697–711.

Wylie, E. B. & Streeter, V. L. 1993 *Fluid Transients in Systems*. Prentice-Hall, Englewood Cliffs, NJ.

First received 8 January 2010; accepted in revised form 31 August 2010. Available online 3 February 2011

APPENDIX

The numerical simulation of the pressure signal, h^t, can be performed by solving numerically the total differential equations of transient flow obtained by means of the Method Of Characteristics (MOC). Focusing the attention on the connection node J (Figure 15) – for further details about the other boundary conditions see Wylie & Streeter (1993) – under the hypothesis of neglecting minor head losses, the energy equation requires a common piezometric head in each segment of the junction. As a consequence, the following condition can be written:

$$h^t_J = h^t_{J,mu} = h^t_{J,md} = h^t_{J,b} \tag{12}$$

where *J,mu* and *J,md* indicate the nodes in the main pipe immediately upstream and downstream of *J*, respectively, and *J,b* is the initial node of the branch.

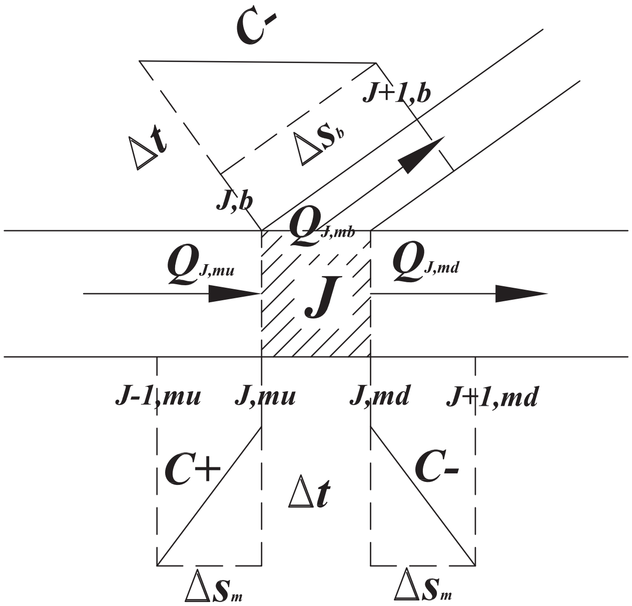

Figure 15 | Connection node scheme.

Furthermore at node *J* the following continuity equation must be satisfied:

$$Q^t_{J,mu} = Q^t_{J,md} + Q^t_{J,b}. \tag{13}$$

Within MOC, the value of h^t_J is given by the following relationship:

$$C^+ : h^t_J = C_{P,m} - B_{P,m} Q^t_{J,mu} \tag{14}$$

as the end node of the main pipe upstream *J*, with C^+ = positive characteristic line, and

$$C^- : h^t_J = C_{N,m} + B_{N,m} Q^t_{J,md} \tag{15}$$

$$C^- : h^t_J = C_{N,b} + B_{N,b} Q^t_{J,b} \tag{16}$$

as the initial node of the main pipe downstream *J* and the branch, respectively, with C^- = negative characteristic line. In Equations (14)–(16)) the coefficients $C_{P,\mathrm{m}}$, $B_{P,\mathrm{m}}$, $C_{N,\mathrm{m}}$, $B_{N,\mathrm{m}}$, $C_{N,\mathrm{b}}$ and $B_{N,\mathrm{b}}$ have the following expressions:

$$C_{P,m} = h^{t-\Delta t}_{J-1,mu} + B_m Q^{t-\Delta t}_{J-1,mu} \quad B_{P,m} = B_m + R_m |Q^{t-\Delta t}_{J-1,mu}| \tag{17}$$

$$C_{N,m} = h^{t-\Delta t}_{J+1,md} - B_m Q^{t-\Delta t}_{J+1,md} \quad B_{N,m} = B_m + R_m |Q^{t-\Delta t}_{J+1,md}| \tag{18}$$

$$C_{N,b} = h^{t-\Delta t}_{J+1,b} - B_b Q^{t-\Delta t}_{J+1,b} \quad B_{N,b} = B_b + R_b |Q^{t-\Delta t}_{J+1,b}| \tag{19}$$

and are known constants since all the values of both *h* and *Q* concern the previous time step; $B_\mathrm{m} = a_\mathrm{m}/gA_\mathrm{m}$ and $B_\mathrm{b} = a_\mathrm{b}/gA_\mathrm{b}$ are the characteristic impedance of the main pipe and branch, respectively; $R_\mathrm{m} = \lambda_\mathrm{m}\Delta s_\mathrm{m}/2gD_\mathrm{m}A^2_\mathrm{m}$ and $R_\mathrm{b} = \lambda_\mathrm{b}\Delta s_\mathrm{b}/2gD_\mathrm{b}A^2_\mathrm{b}$ are the resistance coefficient of the main pipe and branch, respectively; λ = Darcy–Weisbach friction factor, a = pressure wave speed, A = pipe area and g = acceleration due to gravity. At any instant of time, Equations (12)–(16) give the value of the unknowns h^t_J, $Q^t_\mathrm{J,mu}$ $Q^t_\mathrm{J,md}$ and $Q^t_\mathrm{J,b}$ respectively.